

Interpretation of diagram and satellite L -x-ray transitions around $Z = 50$

J. Q. Xu* and E. Rosato

*Dipartimento di Fisica Nucleare, Struttura della Materia e Fisica Applicata—Università di Napoli
and Istituto Nazionale di Fisica Nucleare, Sezione di Napoli, Mostra d'Oltremare pad. 20, I80125 Napoli, Italy*

(Received 6 July 1987)

A simple model, accounting for multiple-hole configurations, is presented in order to study the relative intensities of observed satellite and diagram x-ray lines following L -shell ionization in the region around $Z=50$. Since satellites arising from LN double- and LNN triple-hole states generally are embedded within the natural width of the parent diagram lines and the observed satellites are due to LM and/or LMX ($X=M,N$) multiple-hole states, a clear distinction is drawn among the different multivacancy distributions. Moreover, Coster-Kronig transitions and shakeoff processes, which are responsible for the observed satellite structures, are explicitly taken into account. A new analysis of the L -series x-ray spectra, induced by 2.5-MeV proton bombardment, for elements $Z=47-53$ has been performed based on the present model. L_1 -subshell level widths Γ_1 , fluorescence yields ω_1 , partial Coster-Kronig transition rates f_{13M} , and shakeoff probabilities P_M have been obtained. Present values are in good agreement with recent measurements. However, they show large disagreement with both theoretical calculations and compiled data due to the overestimated intensity and to the assumed sharp cutoff of the $L_1-L_3M_{4,5}$ Coster-Kronig transition rates.

I. INTRODUCTION

The deexcitation modes of L_1 -subshell vacancies for the elements around $Z=50$ are still an intricate and open problem from both an experimental and theoretical point of view. Actually the intensity and the cutoff of the $L_1-L_3M_{4,5}$ Coster-Kronig (CK) transitions are not known with the needed accuracy. CK processes, which produce rearrangement of primary vacancies among subshells of the same major shell, represent the most important decay way whenever they are allowed.¹⁻⁴ The onset and the cutoff of these transitions in certain regions of the Periodic Table strongly influence the initial state lifetimes and, hence, level widths, radiative, and Auger yields.^{1,5}

In recent years much theoretical effort has been devoted to this subject because CK rates and fluorescence yields are necessary for interpreting a large variety of measurements and phenomena. Nevertheless many doubts still persist and we hope for a deeper understanding of L_1 -vacancy decay. Furthermore the experimental information is very scarce except for linewidth measurements.

To give an idea of present knowledge the Ag values of L_1 -subshell level width Γ_1 , fluorescence yield ω_1 and CK rates f_{12} and f_{13} , which represent the probability that an initial $2s$ vacancy is transferred to L_2 and L_3 subshell, respectively, are listed in Table I. The large discrepancy among the different values originates mainly from the assumed sharp cutoff and from the intensity of the $L_1-L_3M_{4,5}$ CK transition.

In fact, trying to explain the Ag L -x-ray spectrum,⁶ McGuire⁷ proposed that the observed L satellites are produced by LN doubly ionized atoms and the $L_1-L_3M_{4,5}$ CK transition is energetically impossible. The agreement of the experimental value of fluorescence yield ω_1 (Ref. 8)

with McGuire's result should be considered somewhat fortuitous, as pointed out by Chen *et al.*,⁹ who reached completely opposite conclusions. Their analysis of the same Ag L -series x-ray spectrum⁶ leads to the following results. The observed satellite structures are due to LM doubly ionized states created by $L_1-L_3M_{4,5}$ CK transitions and by electron shakeoff, while the satellites originating from LN double-hole configurations are hidden within the parent diagram lines. The $L_1-L_3M_{4,5}$ CK processes are energetically allowed in the case of silver; however, the corresponding theoretical rate had to be reduced by a factor of $\sim 1/2.5$ in order to improve the agreement with the experimental results. These results are supported by the relativistic analysis of the $L\alpha$ x-ray satellite spectra for Ag based on the multiconfiguration Dirac-Fock method,¹⁰ although the role of direct multi-

TABLE I. Ag L_1 -subshell level width, fluorescence, and CK yields.

Γ_1 (eV)	ω_1	f_{12}	f_{13}	Ref.
9.03	0.0102	0.052	0.786	12
6.852	0.0114	0.068	0.740	4
7.555	0.0101	0.064	0.695	14
5.3				6
	0.034±0.003			8
2.81	0.0329	0.167	0.313	7
6.17	0.013	0.067	0.730	9 ^a
3.89	0.020	0.107	0.571	9 ^b
4.88	0.016	0.10	0.59	5,24
	0.0188±0.0013	0.121±0.011	0.547±0.055	12

^aFull $L_1-L_3M_{4,5}$ transition rate.

^b $L_1-L_3M_{4,5}$ transition rate reduced to 40%.

ionization is rather overestimated. The same findings have been observed by Putila-Mäntylä and Graeffe,¹¹ who measured L -subshell linewidths for the elements with atomic number $Z=41-51$. Recently a semiempirical evaluation of L_1 -subshell fluorescence yields and CK rates has been performed for the elements ranging from $Z=47$ to 53.¹² The results indicate a Z dependence of the above quantities smoother than theoretical calculations^{4,13,14} and phenomenological compilation.⁵ The agreement with high-resolution measurements of relative intensities of diagram and satellite L lines in the same region of the Periodic Table^{11,15} is excellent.

In this paper a simple model is described for analyzing intensity ratios of satellite and diagram L lines around $Z=50$. The radiative transitions are classified, according to the vacancy distribution of the de-exciting state, into single-, double-, and triple-hole decays. Multiple vacancy configurations are assumed to be produced by shakeoff and CK transitions while direct multiple ionization is considered negligible. The observed high-energy satellites derive from LM double-hole and LMX ($X=M, N$) triple-hole states. Instead the energy shift of satellite L x rays originating from LN and LNN multiple-hole states is insufficient to allow these transitions to be resolved from parent diagram lines also in high-resolution measurements.⁹ The present model is somewhat analogous to the one of Ref. 16, but the latter disregards changes of decay rates with the number of vacancies, except for the radiative rates, during the reorganization process of the atom. On the contrary we explicitly take into account and study the role of possible modifications of both level and radiative widths of L_i subshells in the case of multiple vacancies. Moreover we have directly introduced into our model ionization cross sections in place of the initial vacancy distribution which is unknown *a priori* and, hence, would require several repetitive calculations. Finally, as a straightforward consequence of the model, a clear criterion appears for localizing the cutoff of the $L_1-L_3M_{4,5}$ CK transition around $Z=50$.

The model has been used and checked by analyzing the experimental data of Ref. 15. L_1 -subshell level widths Γ_1 , fluorescence yields ω_1 , partial CK rates f_{13M} , and shakeoff probabilities P_M have been obtained and compared with data available from literature. The agreement

is quite good with recent measurements¹¹ and semiempirical estimates,¹² while a large disagreement appears with both theoretical calculations and compiled values.

II. THEORETICAL MODEL

Satellite x-ray transitions originate when the primary vacancy distribution is modified by electron shakeoff and CK processes to a final multiple-hole configuration. In order to calculate the intensities of satellite and diagram L lines, the following assumptions are made: (a) the relaxation time of atomic core is much shorter than the L_i -hole lifetime;¹⁷ (b) satellites due to LN and LNX ($X=N, 0$) multiple-hole states are not resolved from diagram lines, while the observed satellite structures arise from LM double-hole and LMX ($X=M, N$) triple-hole states;⁹ (c) multiple shakeoff events are neglected.¹⁶

Hence, the shakeoff probabilities and the CK rates are expressed as

$$P_i = P_{iM} + P_{iN} , \quad (1)$$

$$f_{ij} = f_{ijM} + f_{ijN} , \quad (2)$$

in order to separate the contributions from the different configurations. Here P_{iX} is the X -shell electron shakeoff probability due to the L_i -subshell hole and f_{ijX} refers to the L_i-L_jX CK transitions.

The cross sections of the L_i -subshell diagram lines arising from single-hole states are given by

$$\sigma(L_i) = \sigma_i(1 - P_i)\omega_i , \quad (3)$$

whereas for the L_iX ($X=M, N$) double-hole configuration the corresponding expressions are

$$\sigma(L_1X) = \sigma_1 P_{1X} \omega'_{1X} , \quad (4a)$$

$$\sigma(L_2X) = [\sigma_1(1 - P_1)f_{12X} + \sigma_2 P_{2X}] \omega'_{2X} , \quad (4b)$$

$$\sigma(L_3X) = [\sigma_1(1 - P_1)f_{13X} + \sigma_2(1 - P_2)f_{23X} + \sigma_3 P_{3X}] \omega'_{3X} . \quad (4c)$$

Finally, the cross sections for satellite L lines originating from triple-hole states of the type LXY ($X, Y=M$ and/or N) are given by

$$\sigma(L_1XY) = 0 , \quad (5a)$$

$$\sigma(L_2XY) = \sigma_1[(1 - \delta_{XY})(P_{1X}f_{12Y} + P_{1Y}f_{12X})\omega''_{2XY} + P_{1X}f_{12X}\omega''_{2XX}] , \quad (5b)$$

$$\begin{aligned} \sigma(L_3XY) = \sigma_1\{ & [P_{1X}f_{13X} + (1 - P_1)f_{12X}f_{23X}]\omega''_{3XX} \\ & + (1 - \delta_{XY})[P_{1X}f_{13Y} + P_{1Y}f_{13X} + (1 - P_1)(f_{12X}f_{23Y} + f_{12Y}f_{23X})]\omega''_{3XY}\} \\ & + \sigma_2[P_{2X}f_{23X}\omega''_{3XX} + (1 - \delta_{XY})(P_{2X}f_{23Y} + P_{2Y}f_{23X})\omega''_{3XY}] , \end{aligned} \quad (5c)$$

where δ is the Kronecker delta.

Here σ_i are ionization cross sections and unprimed, primed, and doubly primed ω are fluorescence yields for single-, double-, and triple-hole states, respectively. Besides, it is assumed that L_i vacancies always decay before

the outer M holes.

In this framework, the experimentally observed diagram lines contain contributions from pure single-hole and pseudodiagram [Eqs. (5) with $X=Y=N$] transitions. Instead, resolved satellite structures are produced by

multiple-hole states with one M vacancy at least. Therefore, the cross sections of $L\beta_{3,4}$, $L\beta_1$, and $L\alpha$ satellite and diagram lines, are given by, respectively,

$$\sigma_{L\beta_{3,4}}^d = \sigma_1[(1-P_1)\Gamma_{L\beta_{3,4}}/\Gamma_1 + P_{1N}\Gamma'_{L\beta_{3,4}}/\Gamma'_{1N}], \quad (6a)$$

$$\sigma_{L\beta_{3,4}}^s = \sigma_1 P_{1M}\Gamma'_{L\beta_{3,4}}/\Gamma'_{1M}, \quad (6b)$$

$$\begin{aligned} \sigma_{L\beta_1}^d &= \sigma_2[(1-P_2)\Gamma_{L\beta_1}/\Gamma_2 + P_{2N}\Gamma'_{L\beta_1}/\Gamma'_{2N}] \\ &+ \sigma_1[(1-P_1)f_{12}\Gamma'_{L\beta_1}/\Gamma'_{2N} + P_{1N}f_{12}\Gamma''_{L\beta_1}/\Gamma''_{2NN}], \end{aligned} \quad (7a)$$

$$\sigma_{L\beta_1}^s = \sigma_2 P_{2M}\Gamma'_{L\beta_1}/\Gamma'_{2M} + \sigma_1 P_{1M}f_{12}\Gamma''_{L\beta_1}/\Gamma''_{2MN}, \quad (7b)$$

$$\begin{aligned} \sigma_{L\alpha}^d &= \sigma_3[(1-P_3)\Gamma_{L\alpha}/\Gamma_3 + P_{3N}\Gamma'_{L\alpha}/\Gamma'_{3N}] \\ &+ \sigma_2[(1-P_2)f_{23}\Gamma'_{L\alpha}/\Gamma'_{3N} + P_{2N}f_{23}\Gamma''_{L\alpha}/\Gamma''_{3NN}] \\ &+ \sigma_1[(1-P_1)f_{13N}\Gamma'_{L\alpha}/\Gamma'_{3N} + P_{1N}f_{13N}\Gamma''_{L\alpha}/\Gamma''_{3NN}] \\ &+ (1-P_1)f_{12}f_{23}\Gamma''_{L\alpha}/\Gamma''_{3NN}], \end{aligned} \quad (8a)$$

$$\begin{aligned} \sigma_{L\alpha}^s &= \sigma_{L\alpha}^s|_{f_{13M}=0} + \sigma_1 f_{13M}[(1-P_1)\Gamma'_{L\alpha}/\Gamma'_{3M} \\ &+ P_{1N}\Gamma''_{L\alpha}/\Gamma''_{3MN} \\ &+ P_{1M}\Gamma''_{L\alpha}/\Gamma''_{3MM}], \end{aligned} \quad (8b)$$

$$\begin{aligned} \sigma_{L\alpha}^s|_{f_{13M}=0} &= \sigma_3 P_{3M}\Gamma_{L\alpha}/\Gamma_{3M} + \sigma_2 P_{2M}f_{23}\Gamma''_{L\alpha}/\Gamma''_{3MN} \\ &+ \sigma_1 P_{1M}f_{13N}\Gamma''_{L\alpha}/\Gamma''_{3MN}, \end{aligned} \quad (8c)$$

where s and d superscripts indicate observed satellite and diagram lines, respectively; Γ_v and Γ_j denote radiative and level widths, respectively, with the same meaning as above for unprimed and primed quantities; the conditions $f_{12M} = f_{23M} = 0$, which are valid for the concerned elements, have been explicitly used.

With these expressions it is possible to calculate intensity ratios of satellite to diagram x-ray lines and to extract physical information by comparison with experimental measurements. This model is quite general regardless of the ionizing process. Nevertheless the particular ionization mechanism has to be specified in order to compare model predictions with experimental results. Therefore, in the following we shall refer to the case of 2.5-MeV proton bombardment of elements Ag to I, as we shall analyze the experimental data of Ref. 15.

The ECPSSR (Ref. 18) estimates have been used for the L_i -subshell ionization cross sections. This model is a first-order theory which includes corrections for energy loss and Coulomb deflection of the impinging projectile, for the relativistic motion of the inner-shell electrons, and explicitly accounts for orbital polarization and for the increase of binding energy of target electrons. The electron shakeoff probabilities have been derived from the systematics of Ref. 19, according to Slater's recipe,²⁰ which leads to $P_1 = P_2 = P_3$, and are in good agreement with the Ag (Ref. 9) and Zr (Ref. 16) values. The CK rates have been taken from Krause's compilation,⁵ and the partial yields f_{13M} and f_{13N} , have been obtained by adopting the relative ratios of McGuire's estimates,²¹ assuming

$f_{13M}=0$ for $Z > 50$.

For the elements under investigation, additional holes due to CK processes are predominantly created in the N shell for L_1-L_2X and L_2-L_3X transitions, and in $M_{4,5}$ subshells for the L_1-L_3X one. Instead, shakeoff processes mainly produce holes in outer shells, namely $N_{4,5}$. Then most of the M_i and N_i holes ($i=1,2,3$) are transferred to $M_{4,5}$ and $N_{4,5}$ subshells, respectively, by CK transitions.²² Therefore it may be assumed that additional holes are almost exclusively located in these subshells and the L_i -subshell level widths have been evaluated as follows:²³

$$\Gamma'_{iX} = \Gamma_i + \Gamma_{X_{4,5}}, \quad (9a)$$

$$\Gamma''_{iXY} = \Gamma_i + \Gamma_{X_{4,5}} + \Gamma_{Y_{4,5}}, \quad (9b)$$

adopting the values of Refs. 24–27. This scheme will be referred as case II. On the contrary, if $N_{4,5}$ - and $M_{4,5}$ -subshell level widths are assumed negligible with respect to the Γ_i ones, the following relations hold: $\Gamma'_{iX} \approx \Gamma''_{iXY} \approx \Gamma_i$. This situation will be referred as case I. The above hypothesis is well founded for double-hole states, whereas it is rather questionable for triple-hole level widths Γ'' . Anyway, one must bear in mind that the contribution due to terms containing Γ' and Γ'' in Eqs. (6)–(8) is intrinsically small. Therefore such an assumption could be considered correct, as it will be demonstrated by the results later on.

The single-hole radiative widths have been obtained from the theoretical compilation of Scofield.²⁸ The corresponding values for multiple-hole states have been derived according to the approximate Z_{eff}^4 dependence of radiative widths¹⁶ and to the model of Ref. 29.

The calculated intensity ratios of satellite to diagram transitions for $L\alpha$ and $L\beta_1$ x-ray lines are listed in Table II and shown in Fig. 1, together with the experimental results of Ref. 15. The cutoff of the $L_1-L_3M_{4,5}$ CK transition is reproduced quite accurately. However, the trend of the experimental data points is smoother than the calculated values and the agreement between computed and measured relative intensities is rather poor, especially for $Z \geq 50$. The disagreement clearly increases when the $L\beta_1$ transition is considered.

III. ANALYSIS OF RELATIVE INTENSITIES

The cross-section ratios of $L\alpha$ satellites to diagram lines are predominantly governed by $L_1-L_3M_{4,5}$ CK processes for $Z < 50$, while for higher Z elements and for the $L\beta_1$ transitions the relative intensities are almost exclusively determined by electron shakeoff events. Therefore, from inspection of Fig. 1 and Table II the following conclusions may be drawn: (a) The adopted values of electron shakeoff probabilities are too small and (b) the $L_1-L_3M_{4,5}$ CK transition rates are overestimated.

In order to improve the agreement with experimental results and to obtain reliable estimates for the concerned quantities, we continue the analysis of the cross sections. For the sake of clarity we shall limit the discussion to case I, namely L_i -level widths will be assumed constant, regardless of the hole configuration. If these values are

TABLE II. Cross-section ratios of satellites to diagram lines (%).

Z	$L\alpha$			$L\beta_1$		
	Case I	Case II	Ref. 15	Case I	Case II	Ref. 15
47	23.4	21.4	21.1±0.5	1.7	1.5	5.7±0.5
48	23.0	20.9	15.7±0.7	1.5	1.4	6.0±1.0
49	22.6	20.6	15.8±1.5	1.4	1.3	5.7±0.9
50	1.3	1.2	9.8±1.2	1.3	1.2	7.9±0.5
51	1.2	1.1	5.9±0.5	1.2	1.1	5.0±0.5
52	1.1	0.95	7.3±0.7	1.1	0.96	
53	1.1	0.90	7.2±1.2	1.1	0.91	

modified to allow for additional outer holes (case II), the results are almost the same within some percent, except for minor changes of the numerical coefficients which appear in the following formulas. In the framework of constant shakeoff probabilities for the three L subshells, the ratios (σ^s/σ^d) for the $L\beta_1$ and $L\beta_{3,4}$ x rays should be coincident,

$$(\sigma^s/\sigma^d)_{L\beta_{3,4};\beta_1} = 1.1P_M/(1-P + 1.1P_N) \sim 1.1P_M. \quad (10)$$

Moreover, the above-mentioned relative intensities are almost independent on the atomic number, in view of the

$$(\sigma^s/\sigma^d)_\alpha = (\sigma^s/\sigma^d)_{L\beta_1} + 1.1f_{13M}/(1.1f_{13} + 1.1f_{23}\sigma_2/\sigma_1 + \sigma_3/\sigma_1). \quad (12)$$

This equation states that the relative intensity of $L\alpha$ satellite and diagram lines is made up by two different contributions. The first term arises from electron shakeoff events, while the second one is produced by CK transitions. Therefore these relationships constitute a very efficient criterion for localizing the cutoff of the L_1 - $L_3M_{4,5}$ CK transition. Moreover, the same ratios allow

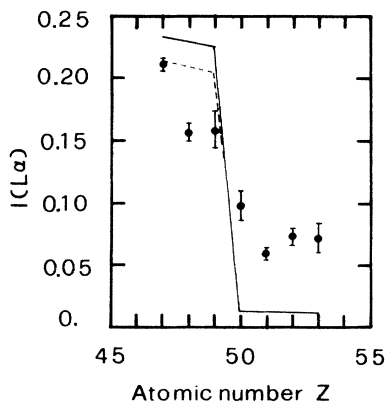


FIG. 1. Relative intensities $I(L\alpha)$ of satellite and diagram $L\alpha$ x rays vs the atomic number Z for 2.5-MeV proton bombardment (—, case I; ---, case II).

very small Z dependence of the shakeoff probability, provided that there are no discontinuities of the L_1 - L_2X CK processes. This condition is verified for $Z \approx 50$ as the closing of the L_1 - $L_2M_{4,5}$ CK transition occurs at $Z=40, 41$.^{11,15}

The same conclusions are valid for the $L\alpha$ transitions whenever the L_1 - $L_3M_{4,5}$ CK processes are forbidden, since in this case

$$(\sigma_\alpha^s/\sigma_\alpha^d)_{f_{13M}=0} = (\sigma^s/\sigma^d)_{L\beta_1}, \quad (11)$$

and hence

to evaluate the partial CK rate f_{13M} .

To check the validity of the model the experimental ratios of total to diagram intensities for $L\alpha$ and $L\beta_1$ lines,

$$R_{L\alpha,\beta_1} = [(\sigma^d + \sigma^s)/\sigma^d]_{L\alpha,\beta_1}, \quad (13)$$

are shown in Fig. 2. As it is evident, $R_{L\alpha}$ decreases

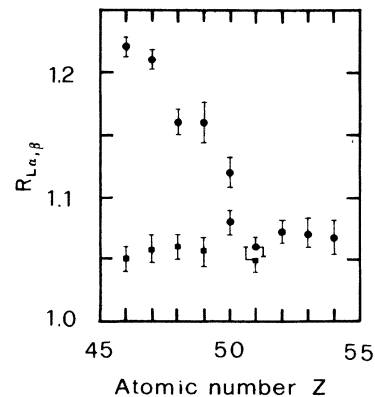


FIG. 2. Ratios $R_{L\alpha,\beta_1}$ of total to diagram cross sections for $L\alpha$ (●) and $L\beta_1$ (■) x-ray emission induced by 2.5-MeV proton bombardment.

TABLE III. Shakeoff probabilities P_M and partial CK yields f_{13M} .

Z	P_M		f_{13M}	
	Case I	Case II	Case I	Case II
47	0.051	0.052	0.374	0.403
48	0.053	0.056	0.250	0.269
49	0.051	0.053	0.260	0.278
50	0.071	0.073	0.045	0.050
51	0.045	0.049	0.023	0.025

smoothly, drops around $Z=50,51$, and then reaches an almost constant value within the experimental errors. Instead, $R_{L\beta_1}$ shows a flat behavior and the plateau value is coincident with the $R_{L\alpha}$ limit for $Z > 50$.

In addition, L_1 -subshell level widths Γ_1 and both total and partial CK transition rates, f_{12} and f_{13} , could be derived from the following expressions and from Eq. (10), (11), or (12) by comparison with the experimental intensity ratios

$$\sigma_{L\beta_1}/\sigma_{L\beta_{3,4}} = (1.1f_{12} + \sigma_2/\sigma_1)\Gamma_1\Gamma_{L\beta_1}/(\Gamma_2\Gamma_{L\beta_{3,4}}), \quad (14)$$

$$\sigma_{L\alpha}/\sigma_{L\beta_{3,4}} = (1.1f_{13} + 1.1f_{23}\sigma_2/\sigma_1 + \sigma_3/\sigma_1) \times (\Gamma_{L\alpha}\Gamma_1)/(\Gamma_3\Gamma_{L\beta_{3,4}}), \quad (15)$$

$$(\sigma_{L\alpha}/\sigma_{L\beta_1})_d = (\sigma_{L\alpha}|_{f_{13M}=0}/\sigma_{L\beta_1})_s. \quad (16)$$

As pointed out elsewhere,¹² these formulas noticeably reduce the contributions to the total error due to uncertainties of the detection efficiency, solid angle, and target thickness measurements. Furthermore, possible inaccuracies of theory in predicting the individual L -subshell ionization cross sections play a minor role, since these quantities are present as relative ratios in the above expressions.

IV. RESULTS AND DISCUSSION

The experimental cross sections for x-ray emission induced by 2.5-MeV proton bombardment¹⁵ have been reanalyzed in terms of the present model by resorting to the radiative widths of Scofield,²⁸ the ECPSSR (Ref. 18) ionization cross sections, and the L -vacancy decay parameters of Krause.⁵ In Table III the present results for M -electron shakeoff probabilities P_M and partial CK yields f_{13M} are listed for the elements ranging from Ag to Sb.

The P_M values have been obtained solely from $L\beta_1$ intensity ratios because the $L\alpha$ satellites are strongly influenced by CK processes. Besides single shakeoff, the quoted results include multiple shakeoff and simultaneous L - and M -shell ionization events. However, these contributions cannot account for the large discrepancy with the computed shakeoff probabilities and with the Ag value of Ref. 9. Although shakeoff processes depend on the ionization mechanism,³⁰ this cannot be invoked to explain the observed differences. On the other hand, the same features have been pointed out for the Ag L -x-ray spectrum⁶ produced by photoionization. In fact, the weak $L\beta_1$ and $L\gamma_1$ satellites were underestimated by a factor of ~ 2 in Ref. 9. This was solely due to a wrong shakeoff probability $P_M \sim 0.02$, since, as already stressed, these satellites are produced by shakeoff events. We find, in the case of 2.5-MeV proton data, almost the same factor of ~ 2 , and this supports our results and interpretation. A definitive conclusion could be drawn from investigation of satellites of $L\beta_{3,4}$ and $L\gamma_{2,3}$ x-ray lines. In this case, multiple-hole configurations are only due to shakeoff processes and the relative intensities could allow us to confirm the present results. In addition, a clear evidence for identical shakeoff probabilities for the L_i subshell could be obtained, besides the arguments previously discussed for the $R_{L\alpha,\beta_1}$ ratios.

Where the partial CK yields f_{13M} are concerned, the

TABLE IV. L_1 -level widths Γ_1 (eV).

Z	Ref. 4	Case I	This work		Ref. 31	Ref. 24	Ref. 11 ^b	
			Case II	Derived ^a				
47	6.85	3.80	4.04	3.68		4.88	3.91	3.27
							(4.4)	(3.7)
48		3.05	3.19	3.07		4.87	3.06	2.87
							(3.7)	(3.4)
49		3.55	3.70	3.55	4.0±0.3	5.00	3.2	3.01
							(3.9)	(3.4)
50	3.00	3.51	3.66	3.32	2.4±0.4	2.97	2.44	2.20
51		2.95	3.04	2.59	2.4±0.3	3.13	2.24	2.13
52	3.26	2.64	2.71		2.5±0.3	3.32		
53		2.44	2.49			3.46		

^aThese data are derived from Γ_2 and Γ_3 values of Ref. 11.

^bThe two series of data refer to $\Gamma_{L\beta_3}$ and $\Gamma_{L\beta_4}$ linewidths measurements, respectively, and are based on the M_{23} level widths of Ref. 26, while the data inside parentheses use values of Ref. 32.

TABLE V. Fluorescence yields ω_1 .

Z	Ref. 9	Ref. 5	Ref. 12	This work	
				Case I	Case II
47	0.0114	0.016	0.0188±0.0013	0.020	0.0188
47	0.020 ^a				
48		0.018	0.0238±0.0016	0.0279	0.0267
49		0.020	0.0276±0.0019	0.0269	0.0258
50	0.0365	0.037	0.0313±0.0026	0.0304	0.0291
51		0.039	0.0359±0.0015	0.0403	0.0391
52		0.041	0.0402±0.0021	0.0501	0.0488
53		0.044	0.0491±0.0011	0.0602	0.0591

^a L_1 - $L_3M_{4,5}$ intensity reduced to 40%.

values are completely reasonable and the agreement with the suggested Ag value⁹ is quite good despite the different ionization mechanism. Furthermore, the same results clearly demonstrate that the L_1 - $L_3M_{4,5}$ transitions is still fully operative up to $Z=49$ and its intensity rather abruptly decreases at $Z=50, 51$.

The L_1 -level widths Γ_1 extracted from the $\sigma_{L\beta_{3,4}}/\sigma_\alpha$ and $\sigma_{L\beta_{3,4}}/\sigma_{L\beta_1}$ ratios are listed in Table IV, together with available experimental measurements,^{11,31} semi-empirical data,²⁴ and theoretical estimates.⁴ Present values derived from $L\alpha$ lines are systematically higher than those corresponding to $L\beta_1$ transitions. This could be ascribed to a somewhat overestimated (underestimated) $L\alpha$ ($L\beta_1$) intensity in Ref. 15. However, present widths are in good agreement with recent experimental

results,¹¹ except for $Z=50$, whose Γ_1 value seems too large. For $Z < 50$ the compiled data of Ref. 24 show a large disagreement with present and experimental results. As a matter of fact, the uncertainties of theoretical and compiled values may become exceedingly high near CK discontinuities and the disagreement could reach a factor of ~ 2 (Refs. 4, 5, and 24). The same features are observed for Γ_2 and Γ_3 values that are systematically higher than measured level widths in this region of the Periodic Table. On the other hand, if measured Γ_2 and Γ_3 values¹¹ are used in place of semiempirical data,²⁴ present results are in excellent agreement with more recent experimental L_1 -level widths. Theoretical calculations are rather scarce and lead to large Γ_1 widths due to the overestimated L_1 - $L_3M_{4,5}$ CK transition rates. Reducing the related intensity by a factor of $\sim \frac{1}{2}$ (Refs. 4 and 11) improves the agreement with the experimental findings.

To further test the model, we have calculated the fluorescence yields ω_1 by using present L_1 -level widths and the radiative widths of Scofield.²⁸ The results are shown in Table V and generally they are in good agreement with our previous estimates,¹² while large discrepancies exist with Krause's data.⁵ The fluorescence yields of Te and I are improbably large since the intensity of the $L\beta_{3,4}$ transition has been most likely overestimated.¹⁵ As already pointed out¹² in this region of the Periodic Table there exist considerable discrepancies between experimental and theoretical values of L -vacancy lifetimes and decay parameters. Therefore highly accurate measurements and a theoretical re-examination are very desirable to clarify the situation.

*Permanent address: Shanghai Institute of Nuclear Research, Academia Sinica, Shanghai, China.

¹W. Bambynek, B. Crasemann, R. W. Fink, H. U. Freund, H. Mark, C. D. Swift, R. E. Price, and P. V. Rao, Rev. Mod. Phys. **44**, 716 (1972).

²M. H. Chen, B. Crasemann, K. N. Huang, M. Aoyagi, and H. Mark, At. Data Nucl. Data Tables **19**, 97 (1977).

³M. H. Chen, B. Crasemann, and H. Mark, At. Data Nucl. Data Tables **24**, 13 (1979).

⁴M. H. Chen, B. Crasemann, and H. Mark, Phys. Rev. A **24**, 177 (1981).

⁵M. O. Krause, J. Phys. Chem. Ref. Data **8**, 307 (1979).

⁶L. G. Parratt, Phys. Rev. **54**, 99 (1938).

⁷E. J. McGuire, Phys. Rev. A **5**, 2313 (1972).

⁸B. Budick and S. Derman, Phys. Rev. Lett. **29**, 1055 (1972).

⁹M. H. Chen, B. Crasemann, M. Aoyagi, and H. Mark, Phys. Rev. A **15**, 2312 (1977).

¹⁰J. Tulkki and O. Keski-Rahkonen, Phys. Rev. A **24**, 849 (1981).

¹¹P. Putila-Mäntylä and G. Graeffe, Phys. Rev. A **35**, 673 (1987), and references therein.

¹²E. Rosato, Nucl. Instrum. Methods B **15**, 591 (1986).

¹³E. J. McGuire, Phys. Rev. A **3**, 587 (1971).

¹⁴B. Crasemann, M. H. Chen, and V. O. Kostroun, Phys. Rev. A **4**, 2161 (1971).

¹⁵B. L. Doyle and S. M. Shafroth, Phys. Rev. A **19**, 1433 (1979).

¹⁶M. O. Krause, F. Wuilleumier, and C. W. Nestor, Jr., Phys. Rev. A **6**, 871 (1972).

¹⁷H. W. Schnopper, Phys. Rev. **154**, 118 (1967).

¹⁸W. Brandt and G. Lapicki, Phys. Rev. A **23**, 1717 (1981).

¹⁹T. A. Carlson, C. W. Nestor, Jr., T. C. Tucker, and F. B. Malik, Phys. Rev. **169**, 27 (1968).

²⁰J. C. Slater, Phys. Rev. **36**, 57 (1930).

²¹E. J. McGuire, Phys. Rev. A **3**, 1801 (1971).

²²E. J. McGuire, Phys. Rev. A **5**, 1043 (1972); **9**, 1840 (1974).

²³J. G. Ferreira, M. O. Costa, M. I. Gonçalves, and L. Salgueiro, J. Phys. (Paris) **26**, 5 (1965).

²⁴M. O. Krause and J. H. Oliver, J. Phys. Chem. Ref. Data **8**, 329 (1979).

²⁵R. A. Pollak, S. Kowalczyk, L. Ley, and D. A. Shirley, Phys. Rev. Lett. **29**, 274 (1972).

²⁶N. Mårtensson and R. Nyholm, Phys. Rev. B **24**, 7121 (1981).

²⁷M. Ohno, P. Putila-Mäntylä, and G. Graeffe, J. Phys. B **17**, 1747 (1984).

²⁸J. H. Scofield, At. Data Nucl. Data Tables **14**, 121 (1974).

²⁹G. Lapicki, R. Metha, J. L. Duggan, P. M. Kocur, J. L. Price, and F. D. McDaniel, Phys. Rev. A **34**, 3813 (1986).

³⁰A. Li-Scholz, A. Leiberich, and W. Scholz, Phys. Rev. A **26**, 3232 (1982).

³¹E. Noreland, Ark. Fys. **26**, 341 (1964).

³²L. I. Yin, I. Adler, T. Tsang, M. H. Chen, D. A. Ringers, and B. Crasemann, Phys. Rev. A **9**, 1070 (1974).